



## Simulating the Early Steps of Amyloid Fibril Formation and Disassembly

Ph. Derreumaux

published in

*From Computational Biophysics to Systems Biology (CBSB08),  
Proceedings of the NIC Workshop 2008,*  
Ulrich H. E. Hansmann, Jan H. Meinke, Sandipan Mohanty,  
Walter Nadler, Olav Zimmermann (Editors),  
John von Neumann Institute for Computing, Jülich,  
NIC Series, Vol. **40**, ISBN 978-3-9810843-6-8, pp. 7-12, 2008.

© 2008 by John von Neumann Institute for Computing  
Permission to make digital or hard copies of portions of this work for  
personal or classroom use is granted provided that the copies are not  
made or distributed for profit or commercial advantage and that copies  
bear this notice and the full citation on the first page. To copy otherwise  
requires prior specific permission by the publisher mentioned above.

<http://www.fz-juelich.de/nic-series/volume40>

# Simulating the Early Steps of Amyloid Fibril Formation and Disassembly

Philippe Derreumaux

Laboratoire de Biochimie Théorique, UPR 9080 CNRS, IBPC, Université 7 Paris-Diderot,  
13 rue Pierre et Marie Curie, 75005, Paris, France  
*E-mail: philippe.derreumaux@ibpc.fr*

More than 20 human diseases are associated with the self-assembly of proteins into transient cytotoxic oligomers and eventually amyloid fibrils. Alzheimer's disease, affecting today more than 15 million people world-wide, is characterized by the aggregation of the  $A\beta(1-40)/A\beta(1-42)$  peptides. Because aggregation is very complex, structural characterization of the intermediate species remains to be determined. Similarly, though N-methylated  $A\beta(16-22)$  peptides inhibit the fibrillogenesis of full-length  $A\beta$  and disassemble fibrils *in vitro*, there is little information about their mechanism of action. Here, I review recent coarse-grained protein simulations aimed at understanding the dynamics and free energy surface of amyloid-forming peptides using the activation-relaxation technique, molecular dynamics and replica exchange molecular dynamics simulations.

## 1 Introduction

Neurodegenerative diseases such as Alzheimer's and prion diseases are characterized by the aggregation of non-related proteins of various amino acid lengths and compositions.<sup>1</sup> There is strong evidence that the soluble oligomers, forming in the early steps of aggregation, are the most cytotoxic species.<sup>2</sup> Structural characterization of these species is difficult, however, experimentally, because they are unstable and span a timescale of several days *in vitro*. One numerical challenge in characterizing these transient oligomers is the development of coarse-grained models and sampling methods able to explore, at an appropriate atomic resolution, large time and spatial scales. Recently, Ma and Nussinov gave a schematic overview over some simulation methods, including all-atom molecular dynamics (MD) simulations in explicit solvent and coarse-grained DMD simulations.<sup>3</sup> All-atom implicit solvent simulations<sup>4-6</sup> and coarse-grained Langevin dynamics<sup>7</sup> are also performed. Here I present recent simulations aimed at understanding the dynamics and free energy surface of amyloid-forming peptides using a coarse-grained implicit solvent protein force field (OPEP) coupled to the activation-relaxation technique (ART), MD and replica exchange MD (REMD) simulations. In an accompanying paper, we present coarse-grained MD and REMD simulations of  $A\beta(16-22)$  oligomers with multiple copies of an N-methylated inhibitor.

The coarse-grained protein simulation package is discussed in Sec. 2, with emphasis on the force field and the benchmarks used for validating the protein model. The results of protein aggregation simulations will be outlined in Sec. 3 and Sec. 4.

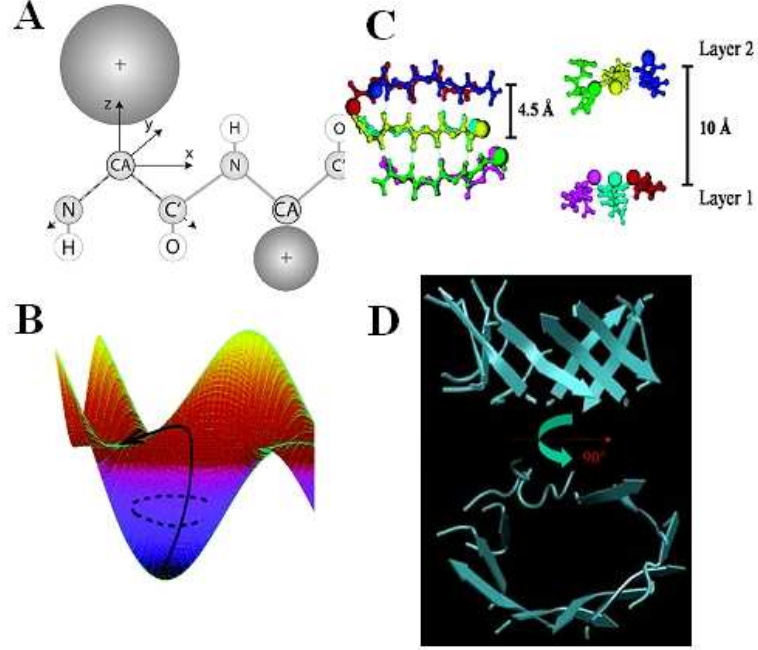


Figure 1. (A) Schematic picture of the coarse-grained model. Most side-chains are represented by a sphere with appropriate radius and physico-chemical property. (B) Sketch of the activation-relaxation technique. Starting from a minimum, the system is subject to a random perturbation and is pushed along the eigenvector of negative eigenvalue until a saddle point is reached, then relaxed to the connecting minimum. (C) A local energy minimum found by ART and MD simulations on A $\beta$ (16-22) hexamer displaying structural characteristics of cross- $\beta$  structure. (D) A representative  $\beta$ -barrel found in MD-OPEP simulations of 16  $\beta$ 2m(83-89) chains starting from a disordered state.

## 2 The Coarse-Grained Protein Simulation Package

### 2.1 OPEP Force Field

The off-lattice model we use consists in a detailed representation of the backbone, modelled by its N, H, C $\alpha$ , C', O atoms and in one bead or centroid for all side-chains, except the proline amino acid which is represented by all heavy atoms (see Fig.1A). OPEP (Optimized Potential for Efficient structure Prediction) version 3.2 is expressed as a sum of local, nonbonded (VdW) and hydrogen-bond (H-bond) terms:<sup>8</sup>

$$\begin{aligned}
 E_{local} = & \sum_{bonds} K_b(r - r_{eq})^2 + \sum_{angles} K_\alpha(\alpha - \alpha_{eq})^2 + \sum_{imp-tors} k_\Omega(\Omega - \Omega_{eq})^2 \\
 & + \sum_{\phi} k_{\phi\psi}(\phi - \phi_o)^2 + \sum_{\psi} k_{\phi\psi}(\psi - \psi_o)^2
 \end{aligned} \tag{1}$$

The term  $E_{local}$  contains force constants associated with changes in bond lengths and bond angles of all particles, changes in improper torsions of the side-chains and the peptide

bonds and changes in  $\phi$  and  $\psi$  angles, where  $\phi_0 = \phi$  within the interval  $[\phi_{\text{lower}}, \phi_{\text{upper}}]$  and  $\phi_0 = \min(\phi - \phi_{\text{lower}}, \phi - \phi_{\text{upper}})$ , otherwise, with  $\phi_{\text{lower}} = -160^\circ$ , and  $\phi_{\text{upper}} = -60^\circ$ , respectively. Similarly, we use  $\psi_{\text{lower}} = -60^\circ$  and  $\psi_{\text{upper}} = 160^\circ$ . Note this analytic form does not prevent sampling of conformations covering all values of  $\phi$  and  $\psi$ .

The nonbonded interactions are modelled by:

$$E_{VDW} = \epsilon_{ij} \left( \left( \frac{r_{ij}^0}{r_{ij}} \right)^{12} - 2 \left( \frac{r_{ij}^0}{r_{ij}} \right)^6 \right) H(\epsilon_{ij}) - \epsilon_{ij} \left( \frac{r_{ij}^0}{r_{ij}} \right)^6 H(-\epsilon_{ij}) \quad (2)$$

Here the Heavyside function  $H(x) = 1$  if  $x \geq 0$  and 0 if  $x < 0$ ,  $r_{ij}$  is the distance between the particles  $i$  and  $j$ ,  $r_{ij}^0 = (r_i^0 + r_j^0)/2$  with  $r_i^0$  the Van der Waals radius of particle  $i$ .

Finally, the  $E_{H\text{-bond}}$  term consists of two-body ( $E_{HB1}$ ) and four-body ( $E_{HB2}$ ) terms:

$$E_{HB1} = \sum_{ij, j=i+4} \epsilon_{hb1-4} \mu(r_{ij}) \nu(\alpha_{ij}) + \sum_{ij, j>i+4} \epsilon_{hb1>4} \mu(r_{ij}) \nu(\alpha_{ij}) \quad \text{with} \quad (3)$$

$$\mu(r_{ij}) = 5 \left( \frac{\sigma}{r_{ij}} \right)^{12} - 6 \left( \frac{\sigma}{r_{ij}} \right)^{10} \quad (4)$$

$$\nu(\alpha_{ij}) = \begin{cases} \cos^2 \alpha_{ij}, & \alpha_{ij} > 90^\circ \\ 0, & \text{otherwise} \end{cases} \quad (5)$$

The sum in eq. (3) is over all residues  $i$  and  $j$  separated by  $j = i + 4$  and  $j > i + 4$  (helices  $3_{10}$  are thus excluded),  $r_{ij}$  is the O..H distance between the carbonyl oxygen and amide hydrogen,  $\alpha_{ij}$  the NHO angle and  $\sigma$ , set to 1.8Å, the equilibrium value of the O..H distance.

Four-body effects, which represent cooperative energies between hydrogen bonds  $ij$  and  $kl$ , are defined by

$$E_{HB2} = \sum \epsilon_{\alpha}^{coop} \exp(-(r_{ij} - \sigma)^2/2) \exp(-(r_{kl} - \sigma)^2/2) \Delta(ijkl) \\ + \sum \epsilon_{\beta}^{coop} \exp(-(r_{ij} - \sigma)^2/2) \exp(-(r_{kl} - \sigma)^2/2) \Delta'(ijkl) \quad (6)$$

with  $\epsilon_{\alpha}^{coop}$  and  $\epsilon_{\beta}^{coop}$  the cooperative energies for  $\alpha$ -helices and  $\beta$ -sheets. The parameter  $\Delta(ijkl)$  is set to 1 if residues  $(k, l) = (i+1, j+1)$  and  $(j = i+4, l = k+4)$ , otherwise  $\Delta(ijkl) = 0$ . Thus helices  $\Pi$  are not stabilized. The parameter  $\Delta'(ijkl) = 1$  if  $k$  and  $l$  satisfy either conditions:  $(k, l) = (i+2, j-2)$  or  $(i+2, j+2)$ ; otherwise  $\Delta'(ijkl) = 0$ .

## 2.2 Sampling Tools

Three sampling tools can be used with the OPEP force field: ART,<sup>9,10</sup> MD<sup>11</sup> and REMD<sup>12</sup>. ART generates trajectories of several thousands of events and brings at each event the system from one relaxed state to another, going through an activation barrier (Fig.1B), and accepts or rejects the move according to the Metropolis criterion. By efficiently crossing energy barriers, ART therefore allows for a rapid sampling of low energy conformations. In contrast to ART, MD, which solves Newton's equations of motion, can explore protein dynamics and REMD, which runs in parallel a series of MD simulations (or replicas) at various temperatures and exchanges them periodically using the Metropolis criterion, can

explore protein thermodynamics. In the applications presented here, the integration time-step is 1 fs,  $T$  is controlled by the Berendsen’s bath and the free energy is calculated using  $F = -RT \log H(x,y)$ , where  $x$  and  $y$  are two reaction coordinates,  $R$  is the gaz constant, and  $H(x,y)$  is the histogram of  $x$  and  $y$ .

### 2.3 Benchmarks

A number of systems have been used to train and validate the OPEP parameters. First, the analytic OPEP form is sufficiently rich to discriminate native from non-native protein structures for 29 targets.<sup>8</sup> Second, the applicability of OPEP in folding was recently revisited on the 60-residue B domain of protein A and we found that ART-OPEP simulations recovered the experimental three-helix bundle starting from random states, but also explained the observed shift to another PDB topology upon mutations.<sup>13</sup> Third, we verified that MD-OPEP describes qualitatively correctly the dynamics of proteins around their native states, although the implicit solvent and the coarse-grained nature of the side-chains modify the clock.<sup>11</sup> Finally, we checked that REM-OPEP reproduces the structural and thermodynamical properties of non-amyloid peptides such as the second  $\beta$ -hairpin from protein G and the 20-residue Trp-cage, starting from randomly chosen states.<sup>12</sup>

## 3 Free Energy Surfaces of Multimers

An important question in protein aggregation is to characterize the free energy surface of small multimers (e.g. dimers or heptamers) because the populated species may represent building blocks for further assembly.

We first probed the free energy surface of the  $A\beta(16-22)$  dimer, resulting from a 50 ns REMD-OPEP simulation starting from two disordered chains in random orientation. We used eight replicas with  $T$  varying between 287 and 500 K with exponential distribution and an exchange time between neighboring replicas of 2 ps, leading to an acceptance ratio between 30%-40%.

The free energy surface at 310 K projected on the cosine of the angle between the two KLVFFAE chains and the extended status of the chains, i.e. the product of the end-to-end distance of the chains divided by the product of the end-to-end distance for two ideal  $\beta$ -strands, shows multiple free energy minima. These are in-register and out-of-register parallel and antiparallel  $\beta$ -sheets, parallel loops and antiparallel loops, and cross conformations. It is interesting that all these states have been described by all-atom REMD simulations in explicit solvent.<sup>14</sup> Overall however, the dimer is found disordered, with a calculated random coil signal of 64% at 310 K.

Does the population of  $\beta$ -sheets change in higher-order species? To this end, we performed 50 MD simulations of 100-300 ns on  $\beta 2m(83-89)$  heptamer at 310 K.<sup>15</sup> Starting from disordered states, we find that amorphous aggregates still represent 65% of the populated states, albeit well-ordered morphologies exist. These include the cross- $\beta$  structure observed experimentally and shown in Fig.1C,<sup>16</sup> with  $C\alpha..C\alpha$  distances of 5.0 Å between the strands and 10.0 Å between the layers, and orthogonal  $\beta$ -sheets with only the meridional 5.0 Å reflection. Of particular interest is the finding of a variety of open and closed  $\beta$ -barrels consisting of six and seven chains with a Boltzmann probability on the order of 10%, i.e. a topology observed for KFFE hexamers<sup>17</sup> and  $A\beta(16-22)$  hexamers<sup>4</sup> using other simulation protocols.

## 4 From Random States to Fibrillar-Like Morphologies

Based on ART-OPEP and MD-OPEP simulations of KFFE,<sup>17</sup> NFGAIL<sup>18</sup> and  $\beta$ 2m(83-89)<sup>19</sup> of various oligomeric sizes (from 6-mers to 16-mers), we could extract a generic aggregation picture of peptides with chain length less than 10 amino acids. Starting from random orientations of the chains and random coil conformations of each chain, the peptides first come together to form amorphous aggregates with a two-stranded or three-stranded  $\beta$ -sheet rapidly in place. Then, the system can remain trapped for a very long time in amorphous aggregates characterized by a total number of side-chain – side-chain and main-chain H-bonding interactions very similar those observed within well-ordered  $\beta$ -sheet structures. Or the system finds pathways to evolve very slowly to transient orthogonal and parallel  $\beta$ -sheets or a variety of closed and open  $\beta$ -barrels. Fig. 1D shows the closed  $\beta$ -barrel obtained from MD-OPEP simulations of 16  $\beta$ 2m(83-89) chains at 310 K and a concentration of 12mM. This  $\beta$ -barrel, which displays an inner diameter of 1.1 nm (minimal interior side-chain – side-chain distance) and is intriguing in terms of cytotoxicity, can be formed from amorphous or orthogonal  $\beta$ -sheets.<sup>15</sup>

## 5 Concluding Remarks

We have described a coarse-grained protein simulation package to study folding and aggregation. The OPEP force field is generic and can be used to study the structural and thermodynamical properties of any amino acid sequence using MD and REMD, or explore the low energy conformations using ART. Based on ART-OPEP and MD-OPEP simulations, we could predict the importance of reptation moves of the chains in the final steps of aggregation, a mechanism later confirmed experimentally.<sup>17</sup> Application of this package to amyloid-forming peptide aggregation can complement experiments by pointing to the non-negligible Boltzmann probability of unexpected topologies, such as the  $\beta$ -barrel. This package is now used to study the aggregation of the A $\beta$ (1-40)/A $\beta$ (1-42) proteins associated with Alzheimer’s disease and fibril disassembly caused by inhibitors, as reported in an accompanying paper.

## Acknowledgments

I am indebted to CNRS, University of Paris 7 and ”ImmunoPrion, FP6-Food-023144, 2006-2009” for financial support. Most of the work was done in collaboration with Normand Mousseau (University of Montreal, Canada), Guanghong Wei (Fudan University, China) and Yasmine Chebaro (CNRS, IBPC, Paris)

## References

1. C. Dobson, *Protein folding and misfolding*, Nature **426**, 884–890, 2003.
2. S. Lesne, M.T. Koh, L. Kotilinek, R. Kaye, C.G. Glabe, A. Yang, M. Gallagher and K.H. Ashe, *A specific amyloid-beta protein assembly in the brain impairs memory*, Nature **440**, 352–7, 2006.

3. B. Ma and R. Nussinov, *Simulations as analytical tools to understand protein aggregation and predict amyloid conformation*, *Curr Opin Chem Biol.* **10**, 445–52, 2006.
4. A. Irback and S. Mitternacht, *Spontaneous beta-barrel formation: an all-atom Monte Carlo study of Abeta16-22 oligomerization*, *Proteins* **71**, 207–214, 2008.
5. J.H. Meinke and U.H. Hansmann, *Aggregation of beta-amyloid fragments*, *J. Chem. Phys.* **126**, 014706, 2007.
6. J. Khandogin and CL. 3rd Brooks, *Linking folding with aggregation in Alzheimer's beta-amyloid peptides*, *Proc Natl Acad Sci U S A.* **104**, 16880–5, 2007.
7. R. Pellerin, E. Guarnera and A. Caffisch, *Pathways and intermediates of amyloid fibril formation*, *J Mol Biol.* **374**, 917–24, 2007.
8. J. Maupetit, P. Tuffery and P. Derreumaux, *A coarse-grained protein force field for folding and structure prediction*, *Proteins* **69**, 394–408, 2007.
9. N. Mousseau, P. Derreumaux, G.T. Barkema and R. Malek, *Sampling activated mechanisms in proteins with the activation-relaxation technique*, *J Mol Graph Model.* **19**, 78–86, 2001.
10. S. Santini, N. Mousseau and P. Derreumaux, *In silico assembly of Alzheimer's Abeta16-22 peptide into beta-sheets*, *J Am Chem Soc.* **126**, 11509–16, 2004.
11. P. Derreumaux and N. Mousseau, *Coarse-grained protein molecular dynamics simulations*, *J. Chem. Phys.* **126**, 025101, 2007.
12. Y. Chebaro, X. Dong, R. Laghei, P. Derreumaux and N. Mousseau, *Replica exchange molecular dynamics simulations of coarse-grained proteins*, in preparation 2008.
13. J.F. Saint-Pierre, N. Mousseau and P. Derreumaux, *The complex folding pathways of protein A suggest a multiple-funnelled energy landscape*, *J. Chem. Phys.* **128**, 045101, 2008.
14. S. Gnanakaran, R. Nussinov and A.E. Garcia, *Atomic-level description of amyloid beta-dimer formation*, *J Am Chem Soc.* **128**, 2158–9, 2006.
15. W. Song, G.H. Wei, N. Mousseau and P. Derreumaux, *Self-Assembly of the beta2-Microglobulin NHVTLQ Peptide Using a Coarse-Grained Protein Model Reveals a beta-Barrel Species*, *J Phys Chem B.* **112**, 4410–8, 2008.
16. Nelson R, Sawaya MR, Balbirnie M, Madsen AO, Riek C, Grothe R, Eisenberg D. Structure of the cross-beta spine of amyloid-like fibrils. *Nature* 2005; 435:773-8.
17. N. Mousseau and P. Derreumaux, *Exploring the early steps of amyloid peptide aggregation by computers*, *Acc. Chem. Res.* **38**, 885–91, 2005.
18. A. Melquiond, J.C. Gelly, N. Mousseau and P. Derreumaux, *Probing amyloid fibril formation of the NFGAIL peptide by computer simulations*, *J. Chem. Phys.* **126**, 065101, 2007.
19. G.H. Wei, W. Song, P. Derreumaux and N. Mousseau, *Self-assembly of amyloid-forming peptides using molecular dynamics simulations and the OPEP coarse-grained force field*, *Front Biosci.* **13**, 5681–5692, 2008.